An efficient computational procedure for random vibro-acoustic simulations

Jean-Pierre Coyette *Karl Meerbergen*

Report TW 482, December 2006

Katholieke Universiteit Leuven
Department of Computer Science
Celestijnenlaan 200A – B-3001 Heverlee (Belgium)

An efficient computational procedure for random vibro-acoustic simulations

Jean-Pierre Coyette *Karl Meerbergen*

Report TW 482, December 2006

Department of Computer Science, K.U.Leuven

Abstract

We discuss a new method for handling random acoustic excitations. The idea is to approximate the cross power spectral density matrix of the response by a low rank matrix. We illustrate the low rank approximation can be computed efficiently by the implicitly restarted block Lanczos method. We give a theoretical explanation.

Keywords : random acoustics, pseudo load cases, Lanczos method.
AMS(MOS) Classification : 62P30, 74S05, 65F15

An efficient computational procedure for random vibro-acoustic simulations

Jean-Pierre Coyette[1] and Karl Meerbergen[2]

[1] Free Field Technologies, 1 rue Francqui, B-1435 Mont-Saint-Guibert, Belgium
[2] Katholieke Universiteit Leuven, Department of Computer Science, Celestijnenlaan 200A, B-3001 Heverlee, Belgium

Keywords: Random acoustics, pseudo load cases, Lanczos method.

Abstract: We discuss a new method for handling random acoustic excitations. The idea is to approximate the cross power spectral density matrix of the response by a low rank matrix. We illustrate the low rank approximation can be computed efficiently by the implicitly restarted block Lanczos method. We give a theoretical explanation.

1 Introduction

Vibro-acoustic simulations often require handling random excitations. This is, for example, the case for acoustic diffuse fields (as encountered in reverberant test chambers) and turbulent boundary layer excitations (as involved in aerodynamic noise studies).

The mathematical framework for modelling such distributed excitations is the concept of (weakly) stationary random process. Such processes are usually characterized, in the frequency domain, by power spectra and are practically defined by referring to a reference power spectrum and a suitable spatial correlation function.

In the time domain, a random process x has a mean zero over one period of time ; the auto-correlation function $R(\tau)$ is the mean value of the product $x(t)x(t+\tau)$ over one period of time. The power spectral density (PSD) is the Fourier transform

of the auto-correlation function and is the characterization of a random process in the frequency domain. If x is a vector of excitations, the random process is determined by the cross power spectral density matrix $S_x(\omega)$. Its (i, j) entry is the cross correlation function for the entries i and j in x respectively. The diagonal elements are the auto correlation functions for the entries of x. The matrix $S_x(\omega)$ is Hermitian positive semi-definite. See [1] [2] [3] [4] [5] for the theoretical background of random processes.

Let in the frequency domain, x be the excitation vector and y the output vector, where $y = Hx$ with H the receptance matrix (the inverse of the dynamic stiffness matrix Z). Then

$$S_y(\omega) = \bar{H}(\omega) S_x H^T(\omega) \ , \tag{1}$$

which is Hermitian positive semi-definite. In a simulation, we are often interested in a few diagonal entries of S_y or the sum of the diagonal entries. In many cases, $Z(\omega) = K - \omega^2 M$ where K, and M are the stiffness and mass matrices respectively. In general, Z is a complex symmetric or unsymmetric matrix. For theoretical reasons, we assume that Z takes the form $K - \omega^2 M$.

In a finite element context, the random excitation x is usually defined on a part of the boundary surface. Let n be the number of dofs in the finite element model and m be the number of dofs along the loaded discrete surface. Usually, $m \ll n$. Then, we could write $S_x = B S_p B^T$ where B is an $n \times m$ prolongation matrix of rank m that maps the excitation dofs onto global dofs, and S_p is an $m \times m$ positive definite matrix. The PSD matrix S_y has dimensions $n \times n$, where n can be very large. Note that it is not feasible storing S_y, since it is a dense matrix of very high dimensions : n can be of the order of $100,000$. On the other hand, S_p can be stored explicitly, since its size is typically much lower, e.g. of the order of $m = 1,000, \ldots, 10,000$. The goal is to approximate

$$S_y \approx W D W^* \quad , \quad D \in \mathbf{R}^{r \times r} \quad , \quad W \in \mathbf{C}^{n \times r} \tag{2}$$

with D a diagonal matrix and r as small as possible. The number of columns of W is the rank of the approximation. Operations on S_y use the factored form (2). In order to reduce the storage and computational costs, we want r to be as small as possible, i.e. $r \ll n$ and if possible $r \ll m$. In this paper, we compare different

techniques. We assume that the multiplication of H is relatively cheap and easy : this assumes an efficient linear system solver with Z.

Here is the plan of the paper. In §2, we present the pseudo load case method, which has shown good performance for low frequencies and in particular for diffuse fields [6]. Experience for turbulent boundary layers using the Corcos [7] and Goody [8] models has shown that r approaches m, especially for higher frequencies, and the computational and storage costs of the method become high. In §4, we present new methods based on the Lanczos method. The motivation is given by the spectral analysis of S_y in §3. Numerical examples using the software ACTRAN [9] are shown in §5.

2 Pseudo load case method

The first technique approximates S_p by the truncated dominant eigendecomposition PDP^* where $D \in \mathbf{R}^{r\times r}$ and $P \in \mathbf{C}^{m\times r}$. Next, we compute $W = \bar{H}(\omega)L$ as the solution of $\bar{Z}W = L$, where $L = BP$ can be considered as a matrix of r pseudo load cases. S_y is then approximated by (2).

This procedure is very efficient when S_p can be approximated by a low rank matrix, and when the computation of P and D is cheap. This assumes that there are only a few large eigenvalues of S_p. Unfortunately, the latter is not really true for turbulent layers or higher frequencies, as we will show by numerical examples.

Computing P and D is not expensive when $r \ll m$. We can use the (block) Lanczos method with implicit restarting [10] [11]. When r approaches m, the Lanczos method is no longer most efficient. In this case, we use the QR method [12], e.g. as implemented in LAPACK [13].

3 Spectral analysis

The spectral properties are best illustrated by an example. Consider some results from a plate excited by a boundary layer following the Corcos model [7]. Figure 1 shows the spectra of S_x and S_y for two frequencies. We notice the following: the

spectrum of S_x becomes denser for the higher frequencies. The spectrum of S_y drops to zero much faster than the spectrum of S_x.

We now give a formal explanation for this behaviour. We assume that Z takes the form

$$Z = U\mathrm{diag}(\zeta_i)U^{-1}$$

where U are the eigenvectors of the undamped eigenvalue problem

$$KU = MU\Omega^2 \tag{3}$$

and

$$\zeta_i = \kappa_i - \omega^2 \ .$$

It is not valid for all applications that we aim to solve, but it gives a sufficient explanation for undamped structures and acoustic cavities.

The matrix S_p becomes more and more diagonally dominant for higher frequencies since the excitation becomes more spatially uncorrelated. This explains why the eigenvalues of S_p lie closer to each other for higher frequencies : it also makes the pseudo load case method more expensive. There is an interesting physical interpretation here : although the excitation is spatially uncorrelated, the response is highly correlated in space, since S_y has a few very large eigenvalues.

An eigenvalue bound can be developed as follows. Define the $n \times m$ matrix $\tilde{B} = \bar{Z}^{-1}B$, then $S_y = \tilde{B}S_p\tilde{B}^*$. Note that $\tilde{B}$ is a rank m matrix. Then, the eigenvalue problem $S_y u = \lambda u$ has exactly m non-zero eigenvalues. Only the non-zero eigenvalues are of interest to us.

Lemma 1 (Reduced Eigenvalue Problem Lemma) *If (λ, u) is an eigenpair of S_y with $\lambda \neq 0$, then λ is an eigenvalue of*

$$\tilde{B}^*\tilde{B}S_p v = \lambda v \ .$$

Proof. It follows that when $\lambda \neq 0$, u lies in the range of $\tilde{B}$: there is a unique v so that $u = \tilde{B}v$. When $\lambda = 0$, it follows that u lies in the nullspace of $\tilde{B}^*$.

Multiplying $S_y u = \lambda u$ on the left by $\tilde{B}^*$ produces

$$\tilde{B}^*\tilde{B}S_p\tilde{B}^*u = \lambda\tilde{B}^*u$$
$$\tilde{B}^*\tilde{B}S_pv = \lambda v$$

with $v = \tilde{B}^*u \neq 0$, which proves the lemma. □

The following lemma may help understand what we see in Figure 1.

Lemma 2 *Let the eigenvalues of $A = \tilde{B}^*\tilde{B}$ and S_y be ordered in descending order. Then*

$$\lambda_j(A)\lambda_m(S_p) \leq \lambda_j(AS_p) \leq \lambda_j(A)\lambda_1(S_p) \ .$$

The spectrum of S_p does not vary in the same way as the spectrum of S_y. The difficulty here is that we do not know the eigenvalues of A. The eigenvalues of A are the squared singular values of $\tilde{B} = \bar{Z}^{-1}B$. Since $\bar{Z}^{-1}B$ is dominated by the modes nearest ω, it is to be expected that the number of large singular values of $\tilde{B}$ is small. Hence, we have

$$\tilde{B} = \sum_{j=1}^{n} \frac{u_j u_j^* B}{\zeta_j} \ . \tag{4}$$

Usually, the sum is made over the terms with smallest ζ_j, i.e. for the κ_j's near ω. This is also the approach that is followed by the modal truncation method. So, we can find an s so that

$$\tilde{B} \approx \tilde{B}_s = \sum_{j=1}^{s} \frac{u_j u_j^* B}{\zeta_j} \ .$$

Define

$$E_s = \sum_{j=s+1}^{n} \frac{u_j u_j^* B}{\zeta_j}$$

so that $\tilde{B} = \tilde{B}_s + E_s$.

If M is a lumped mass, i.e. M is a diagonal matrix, then $u_j^* u_i = 0$ for $j \neq i$. So,

$$\tilde{B}^*\tilde{B} = \tilde{B}_s^*\tilde{B}_s + E_s^*E_s \ .$$

Theorem 1

$$\frac{\|AS_p - \tilde{B}_s^*\tilde{B}_sS_p\|_2}{\|AS_p\|_2} \leq \frac{\|E_s\|_2^2}{\|\tilde{B}_s\|_2^2}\kappa_2(S_p)$$

Proof. For the denominator, note that $\|A\|_2 \geq \|\tilde{B}_s\|_2^2$ since $\tilde{B}_s^*\tilde{B}_s$ and $E_s^*E_s$ are both positive (semi) definite terms. Also, $\|AS_p\|_2 \geq \|A\|_2\sigma_{\min}(S_p)$. For the nominator,

$$AS_p - \tilde{B}_s^*\tilde{B}_sS_p = E_s^*E_sS_p$$

so,

$$\|AS_p - \tilde{B}_s^*\tilde{B}_sS_p\|_2 \leq \|E_s\|_2^2\|S_p\|_2 \ .$$

The proof follows from that $\kappa_2(S_p) = \|S_p\|_2/\sigma_{\min}(S_p)$. □

The theorem tells that if $\tilde{B}$ can be well approximated by a matrix of rank s, so can S_y.

The roles of A and S_p can be interchanged, if S_p can be approximated by a matrix of low rank s.

Since the spectrum of S_y is mainly dominated by the spectrum of A, the spectrum decays as

$$(\kappa_j^2 - \omega^2)^{-2} \ .$$

Let κ_j be ordered following increasing distance to ω. This implies that, if we want an error norm

$$\|S_y - W_rD_rW_r^*\|_2 \leq \tau\|S_y\|_2 \ ,$$

that, roughly speaking, r is determined so that

$$|\kappa_{r+1}^2 - \omega^2|^{-2} \leq \tau|\kappa_1^2 - \omega^2|^{-2} \ .$$

Since the function $(\kappa^2-\omega^2)^{-2}$ decays slower when κ is further away from ω, smaller τ may require a much larger r.

In brief, we can conclude that, *to some extent*, the eigenvectors of (3) play a role in the low rank approximation of S_y in a similar way as modal damping. The situation may be somehow better, since only the modes that have a contribution on the faces with the random excitation, will be taken into account.

4 Lanczos method for S_y

In this section, we show two algorithms using the Lanczos method for computing a low rank approximation of S_y. Since S_y is positive definite, the partial eigende-

composition of rank r is the best approximation to S_y among all matrices with rank r, where the error is measured in the two-norm.

The Lanczos method [14] is an iterative method for the computation of eigenvalues and eigenvectors of a Hermitian matrix. We do not explain the details of this method here, but refer to the literature. In this paper, we use the implicitly restarted block Lanczos method (IRBLM) [10] [11] [15] implemented in ACTRAN [9]. This method computes a relatively small eigenbasis while keeping the memory consumption small. Our implementation uses a stopping criterion that is based on a tolerance on the approximation on S_y. The most expensive operation is the multiplication $Y = S_y X$ where X and Y are matrices with a small number of columns. This requires:

- a solve with Z^T,
- a matrix product with B^T,
- a matrix product with S_p,
- a matrix product with B, and
- a solve with $\bar{Z}$.

The storage requirements can be high, since vectors of size n have to be stored ; this number should be at least $2r$ to make the IRBLM efficient.

The spectrum of S_y consists of $n - m$ zeroes and m positive eigenvalues. We are not interested in the nullspace of S_y. So, if we find an easy way to work with the m dimensional range space only, we reduce the dimension of the problem from n to m and also the size of the Lanczos vectors.

Recall Lemma 1. The eigendecomposition of AS_p is

$$AS_pY = Y\Lambda \tag{5}$$
$$S_yU = U\Lambda \tag{6}$$

where $Y = \tilde{B}^*U$. Multiplication of (5) on the left by $\tilde{B}S_p$ shows that the columns of $\hat{U} = \tilde{B}S_pY$ are eigenvectors of S_y :

$$\tilde{B}S_p\tilde{B}^*(\tilde{B}S_pY) = (\tilde{B}S_pY)\Lambda \ .$$

Since S_y is Hermitian, $U^*U = I$. Since A and S_p are Hermitian positive definite,

$Y^*A^{-1}Y$ and Y^*S_pY are diagonal.

As a conclusion, (5) can be viewed as a symmetric eigenvalue problem in a subspace with inner product $(y, x) = x^*S_py$. This allows us thus to use the Lanczos method with S_p inner product to compute Λ.

Once Λ and Y have been computed, we can compute $\hat{U}$. A normalization is still required to obtain U.

5 Numerical examples

We compare the following methods :

PLQR the pseudo load case method where the QR method is used to decompose S_p,
PLL the pseudo load case method where the Lanczos method is used to decompose S_p,
DL the direct Lanczos method, i.e. the Lanczos method applied to S_y,
RL the reduced Lanczos method, i.e. the Lanczos method applied to AS_p.

5.1 A coarsely discretized problem

The mesh is a quarter cylinder as shown in Figure 2, consisting of 690 solid shell elements and 5138 nodes. The distributed random excitation is related to a turbulent boundary layer acting on the external cylindrical boundary. The number of dofs is $n = 15,414$ and the number of dofs along the randomly loaded boundary is $m = 2,193$. Table 1 shows the rank r for the pseudo load case (PLQR) and the Lanczos (DL) methods in function of the frequency. The rank r was determined so that the error on the rank r approximations to S_p and S_y respectively have a relative error bounded from above by $\tau = 10^{-4}$. For the DL and RL methods, we then have

$$\|S_y - W_rD_rW_r^*\|_2 \leq \tau\|S_y\|_2$$

and for the PLQR and PLL methods, we have

$$\|S_p - P_rD_rP_r^*\|_2 \leq \tau\|S_p\|_2 \ .$$

The computations were carried out on an Opteron running the Suse 9.2 linux operating system. We used the QR method for the decomposition of S_p, since, as you can see from Table 1, r approaches m for the higher frequencies.

From Table 1, we see the impressive difference in r between the two approaches for the same tolerance. Note that there is no visual difference between the results computed by the two methods.

5.2 A finer discretization

For a comparison in performance, we compare the results for the same problem, but with a finer mesh. The mesh consists of 2760 solid shell elements and 19933 nodes. The number of dofs is $n = 59,799$ and the number of dofs along the randomly loaded boundary is $m = 8,525$. We compared the two methods for the frequencies 100 and 400. Table 2 summarizes our results. We used 140 Lanczos vectors in the implicitly restarted block Lanczos method with a block size 5. It is absolutely normal that both Lanczos methods compute the same number of eigenvalues since S_y and AS_p have the same spectrum. The reduced Lanczos method is more expensive, since an additional step is required to compute the eigenvectors of S_y from the eigenvectors of AS_p. An other interesting conclusion, when we compare Tables 1 and 2, is that the number r does not change for the DL method when the mesh is refined. The computation time for the pseudo-load case methods is mainly due to the QR method for PLQR and the Lanczos method for PLL. Note that the PLL method becomes significantly more expensive for higher frequencies.

5.3 Comparison for different tolerances

We compare for the same problem the influence of the tolerance τ. Table 3 compares the ranks and computation times for the PLL and DL methods. We use a low frequency for the PLL method and a large frequency for the the DL method. It follows that the increase of the number of vectors is exponential.

6 Conclusions

The evaluation of the random vibro-acoustic response of mechanical structures has been studied by addressing the specific issues related to the distributed nature of the excitation. Both direct and reduced Lanczos methods have been investigated in this context and show excellent convergence properties for the studied problem. In particular, we found that the direct decomposition of S_y leads to a faster method, requiring a smaller rank than the pseudo load case method.

The conclusions only hold for problems where the pseudo load case method produces a large r. It is an open question whether the proposed method performs better for other types of random excitations than the one used in the numerical example.

References

[1] R. Clough, J. Penzien, Dynamics of structures, McGraw-Hill, Kogakusha, Tokyo, 1975.

[2] I. Elishakoff, Probabilistic methods in the theory of structures, Wiley, New York, 1983.

[3] Y. Lin, Probabilistic theory of structural dynamics, Krieger Publishing Company, Malabar, 1876.

[4] N. Nigam, S. Narayanan, Applications of random vibrations, Springer Verlag, New York, 1994, iSBN 0-387-19861-X.

[5] C. Yang, Random vibrations of structures, Wiley, New York, 1986, iSBN 0-471-80262-X.

[6] J. Coyette, T. Knapen, G. Lielens, K. Meerbergen, P. Ploumhans, Simulation of randomly excited acoustic insulation systems using finite element approaches, ICA Conference, Kyoto, April 4-9, 2004.

[7] C. G.M., Resolution of pressure in turbulence, J. Acoust. Soc. America 35 (2) (1963) 192–199.

[8] M. Goody, An empirical spectral model of surface-pressure fluctuations that includes Reynolds number effects, AIAA Paper 2002-2565, 8th AIAA/CEAS Aeroacoustics Conference and Exhibit, June 17–19 2002, Breckenridge, CO.

[9] Free Field Technologies, MSC.Actran 2006, User's Manual (2006).

[10] D. Sorensen, Implicit application of polynomial filters in a k-step Arnoldi method, SIAM J. Matrix Anal. Applic. 13 (1992) 357–385.

[11] R. B. Lehoucq, D. C. Sorensen, C. Yang, ARPACK USERS GUIDE: Solution of Large Scale Eigenvalue Problems with Implicitly Restarted Arnoldi Methods, SIAM, Philadelphia, PA, USA, 1998.

[12] G. Golub, C. Van Loan, Matrix computations, 3rd Edition, The Johns Hopkins University Press, 1996.

[13] E. Anderson, Z. Bai, C. Bischof, J. Demmel, J. Dongarra, J. Du Croz, A. Greenbaum, S. Hammarling, A. McKenney, S. Ostrouchov, D. Sorensen, LAPACK users' guide, SIAM, Philadelphia, PA, USA, 1995.

[14] C. Lanczos, An iteration method for the solution of the eigenvalue problem of linear differential and integral operators, J. Res. Nat. Bur. Stand. 45 (1950) 255–282.

[15] K. Meerbergen, J. Scott, Design and development of a block rational Lanczos method with partial reorthogonalization and implicit restarting, Technical Report RAL-TR-2000-011, Rutherford Appleton Laboratory, Chilton, Didcot, Oxon OX11 0QX, UK, available through `http://www.numerical.rl.ac.uk/reports/reports.html`. (2000).

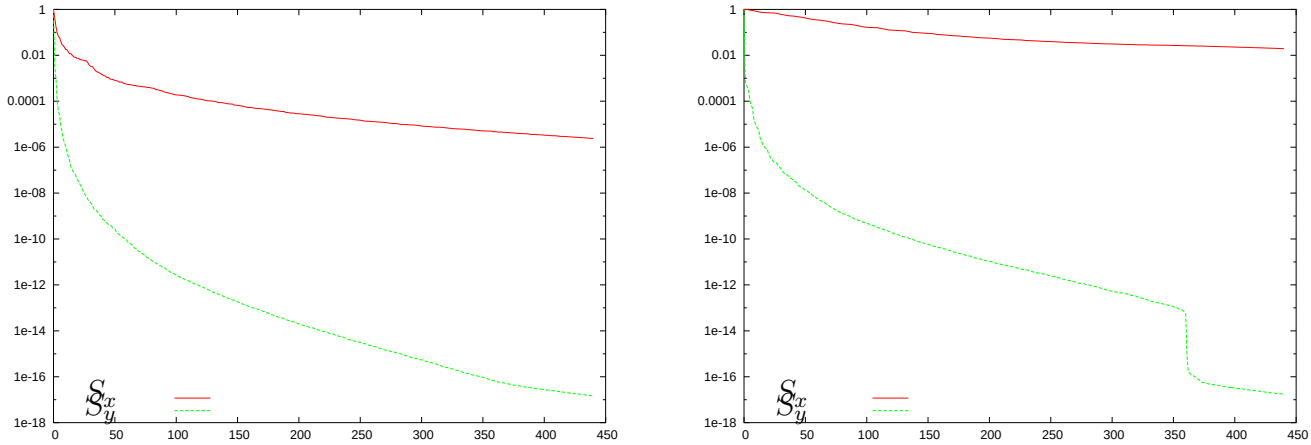

10Hz 200Hz

Fig. 1. Spectra of S_x and S_y for a low frequency and a high frequency

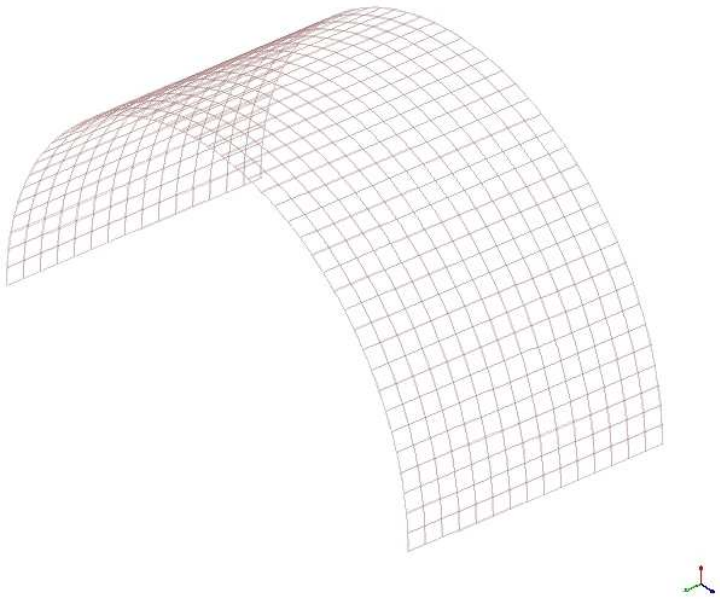

Fig. 2. Mesh of the quarter cylinder

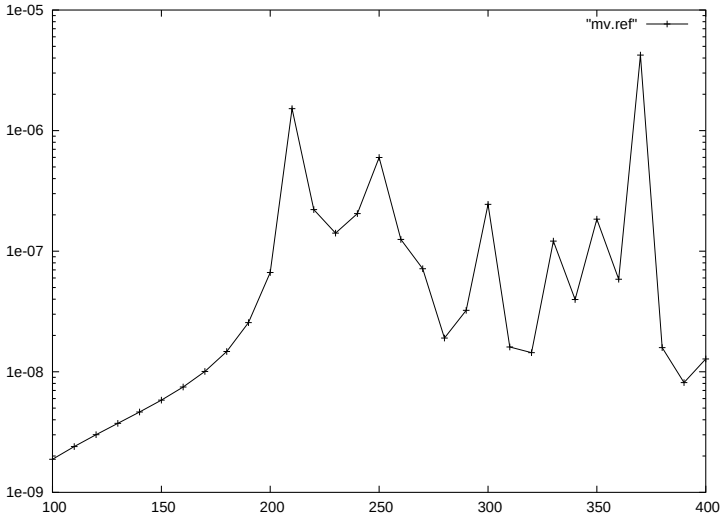

Fig. 3. PSD of mean square velocity

Table 1
Number of rank r for the quarter cylinder problem

frequency	PLQR	DL	frequency	PLQR	DL
100	364	40	250	1015	10
110	411	41	260	1062	24
120	441	40	270	1109	28
130	474	41	280	1155	55
140	512	41	290	1199	40
150	569	41	300	1244	19
160	616	40	310	1297	57
170	648	39	320	1345	63
180	689	36	330	1389	26
190	741	32	340	1444	50
200	793	24	350	1486	23
210	826	7	360	1528	41
220	873	19	370	1589	4
230	928	22	380	1627	69
240	964	21	390	1670	100
			400	1717	77

Table 2
Number of rank r for the quarter cylinder problem

	Pseudo-load methods		Direct methods	
	PLQR	PLL	DL	RL
100Hz				
rank r	425	425	40	40
time (min)	214	16	2.7	5.5
400Hz				
rank r	2383	2383	78	78
time (min)	232	248	3.3	6.3

Table 3
Comparison of r and computation times in function of the tolerance τ

	PLL 100Hz		DL 400Hz	
τ	r	time (min.)	r	time (min.)
10^{-2}	32	2.5	12	2.2
10^{-3}	141	5.0	36	2.8
10^{-4}	425	15.6	78	3.1
10^{-5}	—	—	141	3.1